

## NEW APPROACH FOR A COMBINED PROCESS OF AN ULTRAFAST BORON-OXYGEN DEFECT REGENERATION AND THERMAL CONTACT TREATMENT OF Ni/Cu/Ag PLATED SOLAR CELLS

S. Roder<sup>1</sup>, V. Arya<sup>1</sup>, H. Mir<sup>1</sup>, B. Grübel<sup>1</sup>, S. Kluska<sup>1</sup>, N. Bay<sup>2</sup>, D. Pysch<sup>2</sup>, K. Krauß<sup>3</sup>, A. Brand<sup>1</sup> and J. Nekarda<sup>1</sup>

<sup>1</sup>Fraunhofer Institute for Solar Energy Systems ISE, Heidenhofstr. 2, 79110 Freiburg, Germany

<sup>2</sup>RENA Technologies GmbH, Hans-Bunte-Strasse 19, 79108 Freiburg, Germany

<sup>3</sup>Rehm Thermal Systems GmbH, Leinenstrasse 7, 89143 Blaubeuren, Germany

Phone: +49 761 - 4588 5482; e-mail: sebastian.roder@ise.fraunhofer.de

**ABSTRACT:** A plating sequence of the passivated emitter and rear cell (PERC) concept with Ni/Cu/Ag plated contacts which includes boron-oxygen (BO) defect regeneration and contact annealing is required to ensure a high and light stable efficiency accompanied by a low contact resistance. We introduce an inline-capable process of boron-oxygen (BO) defect regeneration with a simultaneous annealing of the Ni/Cu/Ag plated contact within 10 seconds or less. As basis for the development of the inline capable process a transfer line method (TLM) test structure was used to identify process parameters with respect to time scale, temperature and illumination density. The experimental results demonstrate that an optimized process for simultaneous contact annealing and BO regeneration can achieve a full contact anneal after 1 second and an almost complete BO regeneration after 10 seconds. At higher temperatures above 500 °C a possible shunting through the emitter occurs along with no BO regeneration. Whereas lower temperature of 100 °C slows down contact annealing and BO regeneration significantly to a non-inline practicable process time. Hence, a good process window for complete BO regeneration and contact annealing was observed at a temperature of 250 °C with an illumination density of 27 kW/m<sup>2</sup>. Subsequently, the combined process was successfully transferred to an inline capable tool, which enables a significant speed-up of the contact annealing with simultaneous high BO regeneration. Furthermore, a smaller footprint, no need of nitrogen-rich atmosphere and reduced energy consumption are possible advantages compared to an inline thermal treatment oven for contact annealing.

**Keywords:** contact anneal, plated contact, BO-defect, regeneration, stabilization

### 1 INTRODUCTION

In order to reduce the processing costs of the passivated emitter and rear cell (PERC) concept with Czochralski-grown silicon (Cz-Si); nickel (Ni) - copper (Cu) - silver (Ag) plated contacts warrant a significant reduction in silver consumption compared to screen printed contacts. Further advantages are e.g. reduced contact resistivity on lowly doped emitters [1], smaller contact dimensions (5-15 µm) – leading to less shading losses. In addition, when combined with a selective emitter it leads to potentially higher alignment accuracy due to high flexibility of layer pattern placing. According to the current forecasts of the mass production, it is projected that Ni/Cu/Ag plated cells will have a market share of 10 % by the year 2028 [2]. However, solar cells with plated Ni/Cu/Ag contacts in general have a more complex processing sequence and therefore it is important to simplify process complexity and reduce additional process costs. Furthermore, it is necessary to achieve the full efficiency potential of Cz-Si boron doped PERC cells by suppressing the light-induced degradation (LID) due to boron-oxygen (BO) defects [3]-[6]. Additionally a thermal treatment is known to lower the contact resistance of plated Ni contacts on Si [7] and to be supportive to achieve sufficient adhesion of the plated contact [8]. Thereby the primary aim is to include the BO regeneration and contact annealing process into the standard plating process sequence, in a way, that is optimized to give out best possible results. Whereas a BO regeneration before contact annealing leads to a decrease in efficiency [9]. As the temperature range of the contact annealing and BO regeneration is similar, a combined process would lead to a simplification of the standard plating sequence. Thereby it is necessary to achieve a

good Ni/Cu/Ag contact with a high and stable efficiency within one process.

With the use of a high-power laser technology and an air cooling system we can achieve flexible irradiation intensity and a controllable temperature profile in an offline rapid thermal processing (RTP) oven as well as in a commercially available inline regeneration tool RRS-LID from REHM THERMAL SYSTEMS [10]. Thereby making it possible to combine the process of the BO defect regeneration and the thermal treatment of Ni/Cu/Ag plated cells.

### 2 EXPERIMENTAL

#### 2.1 Setup

An offline laser-based RTP oven is used for heating and excess carrier generation for ultrafast boron-oxygen (BO) defect regeneration and thermal Ni/Cu/Ag contact treatment. The photon energy is 1.27 eV which corresponds to 0.15 eV of excessive energy in silicon at room temperature which will be thermalized. Thereby making it possible to get a high excess carrier injection at elevated temperatures. For a better understanding and transfer to the inline tool it is important to know the time behavior of the respective process. Therefore we use a time resolution of 5 seconds with cognizance of the fact that heating up and cooling down phase may interact with the characteristic of the process. To implement the requested temperature profiles a proportional-integral-derivative (PID) controller adjusts the laser power to certain set temperatures. In Figure 1 the time characteristic of the temperatures with respect to the different set temperatures is shown.

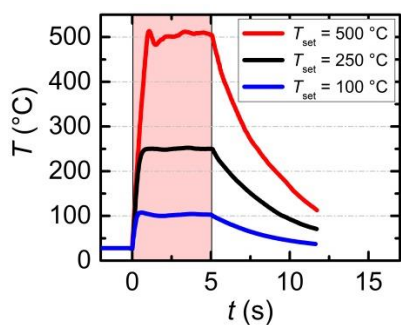


**Figure 1:** Temperature profile of laser-based RTP oven for TLM samples at set temperatures of the PID controller at 100 °C, 250 °C and 500 °C.

The heat up ramp is achieved by a high illumination density. After reaching the set temperature the PID controller downregulates the illumination density to a nearly stable illumination density which corresponds to the set temperature. For instance, heating up to 500 °C, less than 1.2 seconds is needed with an overshoot of  $\pm 20$  °C. It should be noted that different set temperatures result in different illumination densities. Along the cross-sectional view of the sample we can reach temperature homogeneity of  $(100 \pm 1)$  °C,  $(250 \pm 5)$  °C and  $(500 \pm 12)$  °C throughout the process. Furthermore, a hotplate is used as a reference to the offline laser-based RTP oven, as the standard contact annealing is a thermal treatment with low illumination. Whereby, the processes on the laser-based RTP and the hotplate are conducted under a normal atmosphere.

After process development at the offline laser-based RTP oven, we try to transfer the combined process to an inline regeneration tool RRS-LID from REHM THERMAL SYSTEMS. The inline regeneration tool comprises the same laser-based RTP light source as described above and the processes are performed under a normal atmosphere. In addition, an inline thermal treatment oven for contact annealing is used as a reference to the combined process on inline RRS-RLID. The long-lasting reference process must be conducted under a nitrogen-rich atmosphere to prevent corrosion of the fingers, which results in a colour change of the fingers [9].

## 2.2 Sample preparation

For the process development at the offline laser-based RTP oven we use transfer line method (TLM) samples to determine the efficacy of the process with respect to BO regeneration and contact resistance. A TLM stripe has a width of 1 cm, length of 15.6 cm and a finger distance of 1.3 mm which results in 120 fingers. The TLM stripe enables measurement of contact resistance ( $R_C$ ) along with calculation of open-circuit voltage ( $V_{OC}$ ) via a Suns- $V_{OC}$  measurement. In Figure 2 the manufacturing sequence from a boron-doped Cz-Si PERC precursor with a laser contact opening (LCO) at the back-side to a finished TLM stripe is shown. To get access to the investigated parameters a front-side plated contact for TLM measurement and an additional back-side contact for measuring the open-circuit voltage is needed. The aluminum (Al) back-side metallization is realized by screen printing. After the front-side LCO with a width of 15  $\mu$ m, a firing at 850 °C was performed. Therefore we expect that most of the laser damage will

be cured by the firing [11]. Hence, the characteristic of

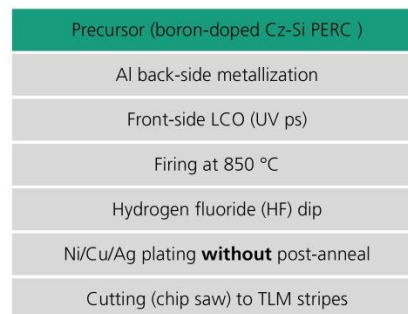


**Figure 2:** Process sequence from boron-doped Cz-Si PERC precursor with a back-side LCO to a finished TLM stripe without standard used post-plating anneal.

the investigated contact anneal and BO regeneration will not be superposed by laser damage annealing. The front-side contact is a Ni/Cu/Ag plated contact which is deposited after a hydrogen fluoride (HF) dip. In Figure 3 the finished TLM sample is illustrated.

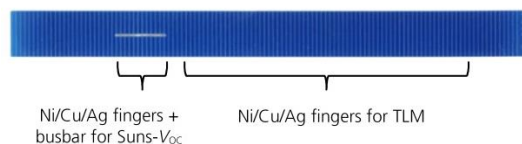


**Figure 3:** TLM sample design with an additional busbar for reproducible contacting and averaging the measured  $V_{OC}$  in this area.

The TLM sample is partitioned in two sections whereby one is the Ni/Cu/Ag plated fingers for TLM measurements (marked on the right side, figure 3) and the other is an additional plated busbar for reproducible contacting and averaging the measured open-circuit voltage. (marked on the left side, figure 3). Furthermore, it is possible to investigate the impact of the plated busbar on the process.

The combined process at the inline regeneration tool is applied on commercial boron-doped Cz-Si PERC Ni/Cu/Ag plated solar cells with a Ni/Cu/Ag front-side grid with 5 busbars and 120 fingers. The back-side is an Al back-side.

## 2.3 Experimental approach

In Figure 4 the experimental approach of the TLM/Suns- $V_{OC}$  sample with the respectively BO state is shown.

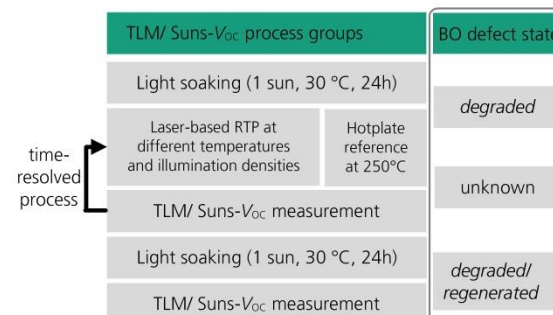


**Figure 4:** Experimental approach (left) and BO defect state (right). As a reference process to the laser-based RTP oven a hotplate is used.

According to a model introduced by Herguth *et al.* [12] BO defects can appear in three different recombination active states (*annealed*, *degraded*, *regenerated*). Thus, it is necessary to transfer the BO defect in a defined state in the beginning without interacting with contact annealing and BO regeneration in order to characterize the effect of the treatment on the BO defect. As the BO defect state after the sample production is unknown we put the BO defect in the *degraded* state with a light soaking step at room temperature under 0.2 suns for 24 hours. The process time is set to 5 seconds with a measurement of the contact resistance ( $R_C$ ) and open-circuit voltage afterwards ( $V_{OC}$ ). Commercially available tools from SINTON and PV-TOOLS were used for measuring  $V_{OC}$  and contact resistance, respectively. The evaluation of the TLM measurement is done with a method based on the compartmentalization of contact resistance and emitter sheet resistance of a TLM network [13]. After a saturation of the target quantity is measured, a light soaking step under 0.2 suns for 24 hours at room temperature is performed in order to test the stability of the BO defects under illumination. Note that the measurements are done in interstitial iron ( $Fe_i$ ) configuration, whereby a Fe-Imaging shows no significant iron concentration. Each process group contains 10 TLM stripes from different wafers of one batch with comparable contact resistance and open-circuit voltage.

To evaluate the efficacy of the combined process on the inline regeneration tool, standard *IV*-measurements and a calculation according to the *pRC* which is introduced by A. Brand *et al.* [9] are done. Whereby the term *pRC* indicates the percentage of *regenerated* BO defects.

### 3 RESULTS

#### 3.1 Offline laser-based RTP and hotplate at 250 °C

A comparison between the offline laser-based RTP and a hotplate as the reference process is performed. In Figure 5 the experimental results for the accumulated process time for the open-circuit voltage and the contact resistance at 250 °C are shown.

At the initial point (0 seconds of processing time) the BO defects exist in *degraded* state with an open-circuit voltage of  $V_{OC,RTP} = (641 \pm 3)$  mV for the laser-based RTP oven (green dots, figure 5) and  $V_{OC,HP} = (640 \pm 1)$  mV for the hotplate (blue triangle, figure 5). After processing for 5 seconds with both the tools, the open-circuit voltage is increased to  $V_{OC,RTP} = (655 \pm 3)$  mV and  $V_{OC,HP} = (655 \pm 5)$  mV which corresponds to an increase of approximately  $\Delta V_{OC} = 15$  mV. After an accumulative process time of 30 seconds, an additional minor increase in open-circuit voltage to  $V_{OC} = (656 \pm 2)$  mV for both tools is observed. As the open-circuit voltage is assumed to not further increase, a light soaking at room temperature under 0.2 suns for 24 hours is applied on the samples. For the groups processed on the hotplate a decrease in  $\Delta V_{OC,HP} = 15$  mV can be detected which matches with the initial value. Therefore, it can be concluded that the hotplate process at 250 °C with no illumination transfers the BO defect from the *degraded* state to the metastable

*annealed* state, as expected due to [14]. A BO reference group, which is annealed at 190 °C for 12 minutes shows an open-circuit voltage increase of  $\Delta V_{OC,Ref} = (15 \pm 2)$  mV from the *degraded* state at  $V_{OC,Ref} = (640 \pm 2)$  mV. For the laser-based RTP oven process a decrease of 1 mV at  $V_{OC,RTP} = (655 \pm 3)$  mV is observed after light soaking. Compared to the annealed BO reference group an increase of  $\Delta V_{OC,RTP} = 14$  mV instead of  $\Delta V_{OC,Ref} = 15$  mV can be achieved along with light stability. Whereas we do not investigated so far if the BO regeneration may be accomplished faster (see section 2.5) as the saturation of the open-circuit voltage is reached after 5 seconds.

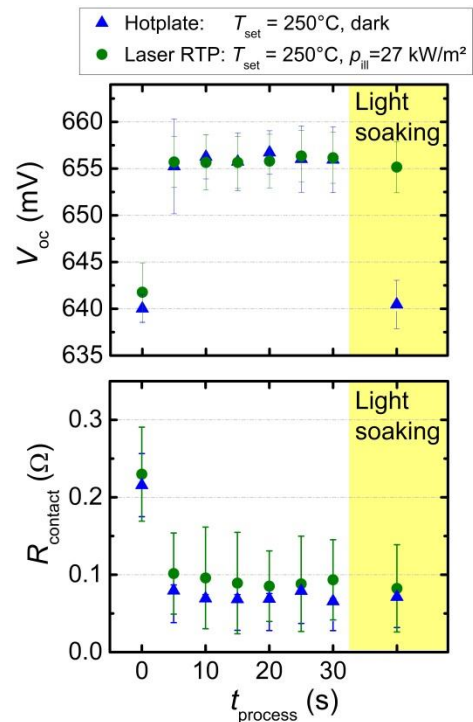


**Figure 5:**  $V_{OC}$  and  $R_C$  over the accumulative process time with a light soaking step at room temperature at 0.2 suns and 24 hours. Process on a laser-based RTP oven and hotplate are compared.

A contrary behavior is observed for the contact resistance. The initial values of contact resistance for the laser-based RTP oven are  $R_{C,RTP} = (0.23 \pm 0.06)$   $\Omega$  and for the hotplate  $R_{C,HP} = (0.22 \pm 0.04)$   $\Omega$ . After a processing time of 5 seconds it is possible to achieve a drop in contact resistance of  $\Delta R_{C,RTP} = 0.13$   $\Omega$  and  $\Delta R_{C,HP} = 0.14$   $\Omega$  (hotplate). A further minor decrease can be seen after the accumulative process time of 30 seconds. After light soaking the contact resistance for the laser-based RTP oven process is at  $R_{C,RTP} = (0.08 \pm 0.05)$   $\Omega$  and for the hotplate process at  $R_{C,HP} = (0.07 \pm 0.02)$   $\Omega$ . To quantify if the hotplate leads to a further reduction in contact resistance, an additional hotplate process after the laser-based RTP oven process at 250 °C for 15 seconds was performed. A further decrease in contact resistance is not observed. Therefore, the contact anneal can be done within 5 seconds and appears to be thermally activated with unknown impact due to the additional illumination. However, a further time-resolved study of the change in contact annealing behavior in response to additional illumination has not

been investigated yet. In future experiments the impact of illumination is planned to be studied.

In summary it is possible to achieve a high BO regeneration within 30 seconds and a lowering in contact resistance within 5 seconds at 250 °C at an illumination density of 27 kW/m<sup>2</sup>. In the next section 2.5 the behavior at the limits of the process will be shown.

### 3.2 Offline laser-based RTP process at process limits

To find the limits of the process with respect to time and temperature, we apply two processes; (i) with an illumination density of 10 kW/m<sup>2</sup> at 100 °C and (ii) with an illumination density of 81 kW/m<sup>2</sup> at 500 °C. Furthermore, to see if it is possible to speed up the BO regeneration a process with an illumination density of 27 kW/m<sup>2</sup> at 250 °C is performed for 10 seconds with a step resolution of 1 second.

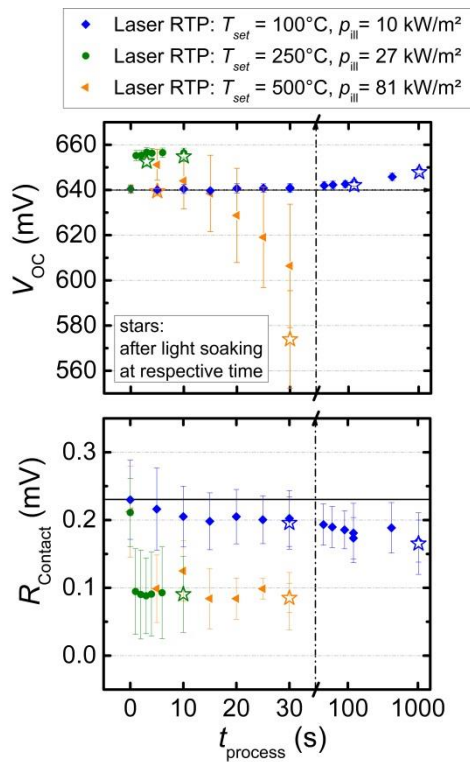


**Figure 6:**  $V_{\text{OC}}$  and  $R_{\text{C}}$  of a combined laser-based RTP oven process at different set temperatures and illumination densities for 100 °C and 500 °C in 5 seconds resolutions and 250 °C in 1 second resolution. Stars represent an additional light soaking after the respective processing time.

In Figure 6 (top) the open-circuit voltage over the process time is shown. As mentioned prior the BO defects are transferred to the *degraded* states with light soaking before the process. This results in  $V_{\text{OC},100^\circ\text{C}} = (640 \pm 1) \text{ mV}$  for 100 °C (blue rhombus),  $V_{\text{OC},250^\circ\text{C}} = (641 \pm 2) \text{ mV}$  for 250 °C (green dot) and  $V_{\text{OC},500^\circ\text{C}} = (640 \pm 2) \text{ mV}$  for 500 °C (orange triangle). The stars in figure 5 represent an additional light soaking after the respective processing time. At a process temperature of 100 °C at 1000 seconds a light stable  $V_{\text{OC},100^\circ\text{C}} = (647 \pm 1) \text{ mV}$  with a difference of  $\Delta V_{\text{OC},100^\circ\text{C}} = 8 \text{ mV}$  to the BO annealed reference group can be reached. Therefore, the BO regeneration was not

fully complete because the BO regeneration rate is relatively low at 100 °C when compared to higher temperatures [15]. Same slowed down behavior can be observed for contact annealing with a decrease in contact resistance to  $R_{\text{C},100^\circ\text{C}} = (0.16 \pm 0.04) \Omega$  after 1000 seconds. As the contact anneal seems to be thermally activated with activation energy, a slowed down kinetics seems to be consistent.

At a process temperature of 250 °C the open-circuit voltage saturates after 3 seconds to  $V_{\text{OC},250^\circ\text{C}} = (656 \pm 2) \text{ mV}$  with a light soak stability of  $V_{\text{OC},250^\circ\text{C}} = (653 \pm 2) \text{ mV}$ . The process is continued to an accumulative processing time of 10 seconds. An open-circuit voltage drop after light soaking of  $\Delta V_{\text{OC},250^\circ\text{C}} = 1 \text{ mV}$  is detected which is equally achievable at a process time of 30 seconds. Contact resistance follows the same trend as in Figure 5 at 250 °C and furthermore the contact anneal can be accomplished within the first seconds of the annealing process.

For higher temperatures above 500 °C, an open-circuit voltage increase is noticed but with an instability under illumination. Therefore, it appears the annealing reaction and the destabilizations of *regenerated* states are dominant at elevated temperatures. For longer process times the open-circuit voltage drops to  $V_{\text{OC},500^\circ\text{C}} = (606 \pm 27) \text{ mV}$  whereby the possible root cause of that is discussed in the next subsection. A decrease in contact resistance to  $R_{\text{C},500^\circ\text{C}} = (0.08 \pm 0.04) \Omega$  within 5 seconds is observed. It is postulated that the contact anneal at 500 °C is additionally accelerated compared to lower temperatures as the contact anneal at 100 °C is significantly slower with regards to the unknown impact of the illumination

### Shunting problems

For a laser-based RTP oven process at 500 °C a decrease in open-circuit voltage can be observed after 10 seconds for any sample with respect to an open-circuit voltage measurement at the busbar. Along with modifications in optics and most likely the build-up of new traps by Ni-spikes [16] in the space charge region, bulk and emitter could be the factors. For further investigations photoluminescence (PL) images before and after the treatment are shown in figure 7.

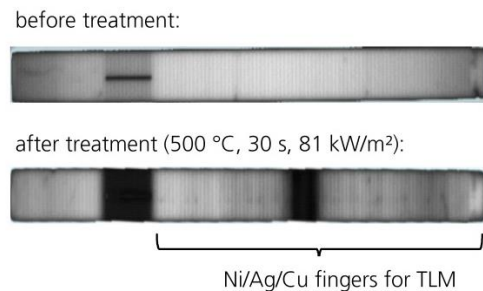


**Figure 7:** Photoluminescence (PL) images before (top) and after a treatment for 30 seconds at 500 °C and 81 kW/m<sup>2</sup> (bottom) under 1 sun PL excitation. Busbar and some TLM fingers show low PL signal after the process.

The PL image before the treatment shows a lower PL signal near the busbar compared to the TLM fingers, which is due to a higher recombination of the excess carrier through laser damage and/ or shadowing of the PL excitation on the busbar. However, a uniform PL signal is measured in the area around busbar and TLM fingers.



After processing at 500 °C for 30 seconds a decrease in PL signal can be observed near the busbar and one section in the TLM array. A decrease in PL signal can be due to high recombination in the bulk or at the connecting interfaces to the bulk. Furthermore, the PL signal is dependent on the local voltage whereby a shunt abruptly decreases the voltage of all the electrically connected contacts. Hence, a shunt will decrease the PL signal along the finger and the busbar which can be seen in Figure 7. In figure 8, a sweep over the TLM fingers is done with the Suns- $V_{OC}$  to measure the open-circuit voltage and subsequently calculated pseudo fill factor ( $pFF$ ) for each finger.

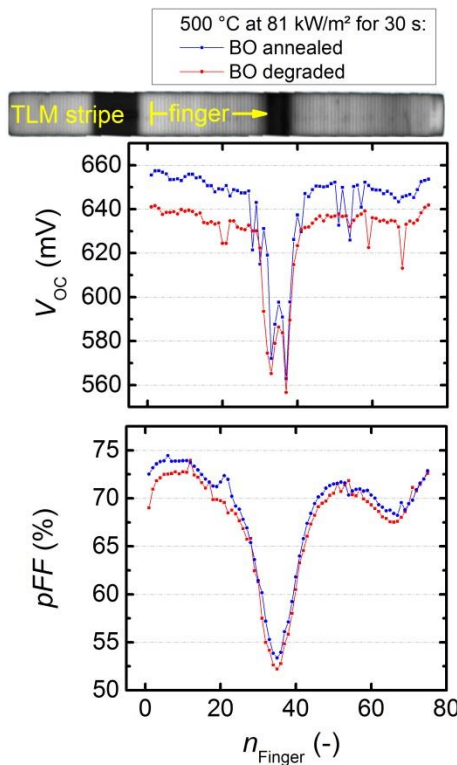


**Figure 8:**  $V_{OC}$  (top) and  $pFF$  (bottom) for TLM fingers after a treatment at 500 °C and an illumination density of 81 kW/m<sup>2</sup> for 30 seconds in the BO *annealed* and BO *degraded* state. As eye guide the PL image of the TLM stripes with a marked arrow for the direction of the measured fingers is shown.

In Figure 8 (top) the measured open-circuit voltage for every finger is shown. Between the finger 1 to 25 and 45 to 78 an open-circuit voltage of  $V_{OC} = 640$  mV in the degraded BO state is measured. After BO annealing an increase of  $\Delta V_{OC} = 15$  mV is observed which corresponds to the previous open-circuit voltage increase in section 3.1 (figure 5). Hence, for those fingers no additional degradation with respect to the BO is observable. Between the finger 26 to 44 a drop to a minimum of  $V_{OC} = 558$  mV is calculated. Same behaviour is seen with  $pFF$  where a drop to a minimum of 52 % can be measured. The decrease in  $V_{OC}$  and  $pFF$  can be seen on the same position in the PL image. The drop in  $pFF$  can be due to traps in space charge region or reduction of the parallel resistance due to shunts [17]. A shunt through the emitter due to Ni-spikes is one of the major reasons for a reduced  $pFF$  and  $V_{OC}$  in Ni/Cu/Ag plated cells with a

high temperature treatment, as shown in [16]. Hence, a process above 500 °C can as well achieve the contact annealing but goes along with non-BO regeneration and an increase in the possibility of shunting through the emitter.

### 3.3 Transfer to inline RRS-RLID

As contact annealing and BO regeneration are achievable within 10 seconds, we transfer the process to an inline regeneration tool. The process is done at a belt speed of 400 cm/min (processing time of 10 seconds) with an illumination density of 24 kW/m<sup>2</sup> and a maximum peak temperature of 270 °C under normal atmosphere. Whereby, the reference process is done on an inline thermal treatment oven with a processing time of 2 minutes at 225 °C under a nitrogen-rich atmosphere. In Figure 9 the results of the  $IV$ -measurements before the process as out-of-box (oob) and after the process with a following light soaking (stab) are shown.

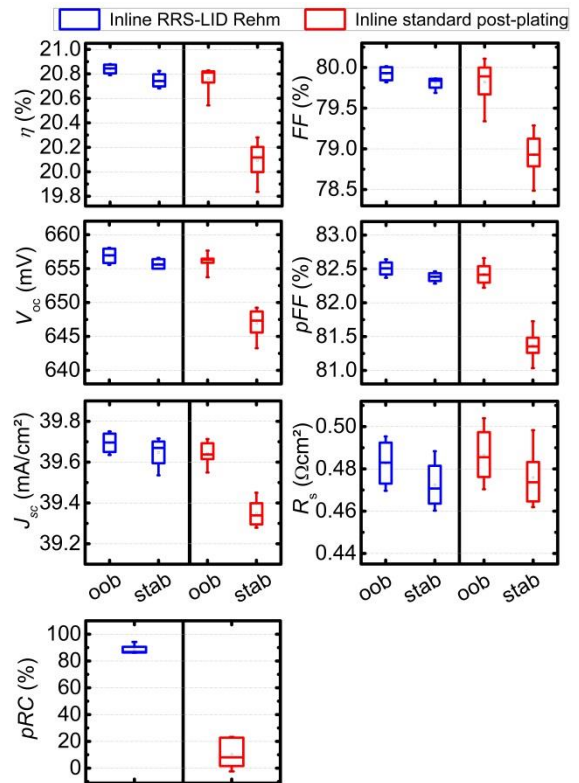


**Figure 9:**  $IV$ -measurement characteristic for evaluation of the combined process. Solar cells are measured right after plating sequence as out-of-box (oob) and after the process and an additional light soaking step as stability test of the BO regeneration. Inline RRS-LID (blue) and inline thermal treatment (red).

A practical characteristic for evaluation of the process represents the efficiency which is approximately at 20.8 % before the process. After the process followed by light soaking at room temperature under 0.2 suns and 24 hours, a decrease of 0.1 %abs for the RRS-LID process and 0.8 %abs for the inline thermal treatment is visible. Similar behaviour is observed for  $V_{OC}$ ,  $FF$ ,  $pFF$  and  $J_{sc}$ . In addition to being a bulk lifetime limiting defect, a BO defect acts as a trap in the space charge region as well; thus affecting  $V_{OC}$ ,  $FF$ ,  $pFF$  and  $J_{sc}$ . For

the inline RRS-RLID a  $pRC$  of 92 % and a  $pRC$  of 10 % is calculated for the inline thermal treatment. Therefore, it is possible to achieve a high BO regeneration > 90 % on the inline RRS-LID within a process time of 10 seconds.

Standard  $IV$ -measurements with a calculation of total series resistance ( $R_S$ ) are used as a basis for discussion to estimate the efficacy of the contact anneal. As  $R_S$  includes all the series resistances of a solar cell, it is assumed that the metal-semiconductor contact at the back-side, base and emitter resistance do not change during the process since they were already exposed to a high temperature firing step at 850°C. A similar decrease in series resistance of 0.01  $\Omega\text{cm}^2$  can be observed for both inline tools. With the previous assumption and that the temperature in the inline RRS-LID is 4 seconds above 250 °C, it is presumed that the decrease in  $R_S$  is due to the contact anneal as determined in section 2.5; contact anneal for laser-based RTP oven is achievable within seconds at 250 °C.

For both tools no change in finger colour is observed, whereby the reference process is conducted under a nitrogen-rich atmosphere.

Hence, in addition to the combined process with full contact annealing and high BO regeneration a significant decrease in processing time is achieved compared to an inline thermal treatment. Furthermore, possible advantages include a smaller footprint, no need of nitrogen-rich atmosphere and reduced energy consumption.

#### 4 CONCLUSION

We have shown that on boron-doped Cz-Si PERC Ni/Cu/Ag plated TLM stripes, the combined process of BO regeneration along with contact anneal is achievable within 10 seconds at a temperature of 250 °C and an illumination density of 27 kW/m<sup>2</sup>. At lower temperatures the contact annealing and BO regeneration reaction is slowed down. Whereas higher temperatures support a faster contact annealing but accompanies at 500 °C with shunting through the emitter. Furthermore, no BO regeneration is reached at 500 °C as the BO annealing reaction and destabilization of BO regenerated states appears to be prominent.

Subsequently, the process was transferred to an inline regeneration tool RRS-LID at a maximum temperature of 270 °C, an illumination density of 24 kW/m<sup>2</sup> and a belt speed of 400 cm/min which corresponds to a process time of 10 seconds. Thereby achieving a BO regeneration of  $pRC > 90$  % on commercial boron-doped Cz-Si PERC Ni/Cu/Ag plated solar cells. Furthermore, a speed-up of the contact anneal with regarding of a decrease in  $R_S$  could be observed for a 10 second process on RRS-LID tool whereas the reference thermal treatment was applied for 2 minutes. Hence, an industry-ready inline-capable process on the RRS-LID tool is found that significantly decreases process time for contact annealing and additionally allows regeneration of BO defects without adding additional tools or process time.

#### 5 ACKNOWLEDGMENT

The authors would like to thank their colleagues at the Fraunhofer institute for solar energy systems (ISE),

RENA and REHM for their help with the experiments and solar cell characterization. This work was funded by the German Federal Ministry for Economic Affairs and Energy within the research project “UFO” and “Genesis” under contract number 0324080 and 032474, respectively.

#### 6 REFERENCES

- [1] S. Kluska, J. Bartsch, A. Büchler, G. Cimiotti, A. A. Brand, S. Hopman, M. Glatthaar, “Electrical and mechanical properties of plated Ni/Cu contacts for Si solar cells”, *Energy Procedia*, 77, pp. 733 – 743, 2015.
- [2] International Technology Roadmap for Photovoltaic (ITRPV), *ITRPV Ninth Edition*, 2018.
- [3] H. Fischer and W. Pschunder, “Investigation of photon and thermal induced changes in silicon solar cells,” *Photovoltaic Specialists Conference, 10th, Palo Alto, Calif.*, pp. 404–411, 1974.
- [4] S. Glunz, S. Rein, W. Warta, J. Knobloch, and W. Wettling, “On the degradation of Cz-silicon solar cells,” *Proc. 2nd WC PVSEC*, 1998.
- [5] K. Bothe, R. Sinton, and J. Schmidt, “Fundamental boron-oxygen-related carrier lifetime limit in mono- and multicrystalline silicon,” *Prog. Photovolt. Res. Appl.*, vol. 13, no. 4, pp. 287–296, Jun. 2005.
- [6] T. Niewelt, J. Schon, W. Warta, S. W. Glunz, and M. C. Schubert, “Degradation of Crystalline Silicon Due to Boron–Oxygen Defects,” *IEEE J. Photovolt.*, vol. 7, no. 1, pp. 383–398, Jan. 2017.
- [7] K. Maex and M. Van Rossum, “Properties of metal silicides”, *Institution of Engineering and Technology*, 1995.
- [8] A. Mondon, M. N. Jawaid, J. Bartsch, M. Glatthaar, S. W. Glunz, “Microstructure analysis of the interface situation and adhesion of thermally formed nickel silicide for plated nickel–copper contacts on silicon solar cells”, *Sol. Energy Mater. Sol. Cells*, 177, pp. 209–213, Apr. 2013.
- [9] B. Gruebel, G. C. Theil, S. Roder, T. Niewelt, S. Kluska, „Impact of Post-Plating Annealing on the Metastable Defect of Boron Doped PERC Solar Cells“, to be published 2019.
- [10] A. A. Brand, K. Krauss, P. Wild, S. Schörner, S. Gutscher, S. Roder, S. Rein, J. Nekarda, “Ultrafast in-line capable regeneration process for preventing light induced degradation of boron-doped p-type Cz-silicon PERC solar cells”, *Proceedings of the 33rd European Photovoltaic Solar Energy Conference*, 2017.
- [11] V. Arya, S. Gutscher, S. Kluska, F. Meyer, G. Cimiotti, J. Nekarda and A. A. Brand, “Improvement of Solar Cell Efficiencies for Ultrashort-Pulse Laser Contact Opening with Ni-Cu Plated Contacts by Optimized LCO-FFO Processing Order,” *Proceedings of 35th European Photovoltaic Solar Energy Conference and Exhibition*, pp. 805 - 809, 2018.
- [12] A. Herguth, G. Schubert, M. Kaes, and G. Hahn, “Avoiding boron-oxygen related degradation in highly boron doped Cz silicon,” *Proceedings of the 21st European Photovoltaic Solar Energy Conference*, pp. 530–537, 2006.

- [13] H. Mir, V. Arya, H. Hoeffler, A. A. Brand, "A Novel TLM Analysis for Solar Cells", *IEEE Journal of Photovoltaics*, July 2019.
- [14] G. Hahn, S. Wilking and A. Herguth, "BO-related Defects: Overcoming Bulk Lifetime Degradation in crystalline Si by Regeneration", *Solid State Phenomena*, 242, S.90-89, 2016.
- [15] A. Herguth, C. Derricks and G. Hahn, "Regeneration of boron-oxygen related degradation in Cz-Si PERC-Type solar cells at high temperatures", *Proceedings of the 33rd European Photovoltaic Solar Energy Conference*, pp. 557–560, 2017.
- [16] A. Buechler, S. Kluska, M. Kasemann, M. Breitwieser, W. Kwapil, A. Hähnel, H. Blumtritt, S. Hopman, M. Glatthaar, "Localization and characterization of annealing-induced shunts in Ni-plated monocrystalline silicon solar cells", *Phys. Status Solidi RRL* 8, No. 5, 385–389, 2014.
- [17] S. Glunz, "Ladungsträgerrekombination in Silizium und Siliziumsolarzellen", Dissertation, *Albert-Ludwigs-Universität Freiburg*, 1995.